JOURNAL OF GUIDANCE, CONTROL, AND DYNAMICS
Vol. 20, No. 1, January–February 1997

Comparison of Master Station and User Algorithms for Wide-Area Augmentation System

Changdon Kee,* Todd Walter,† Yi-chung Chao,‡ Yeou-Jyh Tsai,§ Per Enge,¶ and Bradford W. Parkinson**
Stanford University, Stanford, California 94305-4085

The global positioning system will be used for a wide variety of applications. However, aircraft use of any satellite-based navigation system raises significant concern with respect to accuracy and integrity. The wide-area augmentation system (WAAS) is a navigation system that adds an independent ground network and increases navigation accuracy and integrity. The WAAS will be a supplemental navigation aid for all phases of flight down to category I precision approach in 1997. Eventually, it will be a primary navigation aid. Stanford University installed three wide-area reference stations in the Western United States and has been conducting independent flight tests of WAAS since 1994. The comparison of the two different WAAS algorithms and the results from the Stanford University WAAS static and flight tests are presented. The results showed that 3.5 m of WAAS user vertical positioning accuracy, compared to 80 m for stand-alone, can be achieved using both WAAS algorithms. That accuracy is within the ±4.1-m 95% error limits for a category I instrument landing system. An improvement on the existing grid ionosphere estimation algorithm is also included as well as the introduction of a weighted least-square solution in WAAS user position computation.

Nomenclature

B_i = ith wide-area reference station's (WRS's) clock error
$B_{i,n}$ = ith WRS's clock error relative to nth WRS's clock
$\hat{B}_{i,n}$ = estimate of ith WRS's clock error relative to nth WRS's clock
b^j = jth satellite selective availability (SA)
$\tilde{b}^j$ = jth satellite clock error (including SA)
d_i^j = physical distance from ith WRS to jth satellite
d^k = distance from kth pierce point to the grid
$\boldsymbol{e}_i^j$ = range unit vector from ith WRS to jth satellite
$I_{\text{Klob},V}^{\text{Grid}}$ = broadcast Klobuchar vertical ionospheric delay at the grid point
$I_{\text{Klob},V}^k$ = broadcast Klobuchar vertical ionospheric delay at the pierce point
$I_{\text{Meas},V}^k$ = measured vertical ionospheric delay at the pierce point
$\hat{I}_{\text{Grid},V}$ = estimated vertical ionospheric delay at the grid point
i_i^j = ionospheric time delay from jth satellite to ith WRS
K = total number of the ionosphere pierce points
$l_{i,n}$ = number of common satellites in view from ith and nth sites
m_i^j = multipath from jth satellite to ith WRS
$\boldsymbol{R}_u$ = location vector from Earth center to user
t_i^j = tropospheric delay from jth satellite to ith WRS
v_i^j = measurement noise from ith WRS to jth satellite including multipath error
w^k = weight for the kth pierce point
$\delta B_{i,n}$ = ith WRS's time synchronization error because of ephemeris error and measurement noise
$\delta \boldsymbol{R}^j$ = ephemeris error vector of the jth satellite
$\delta\rho_i^j$ = pseudorange residual already adjusted for broadcast ephemeris and satellite clock and atmospheric error
η_i^j = measurement noise
ρ_i^j = pseudorange from ith WRS to jth satellite
$\sigma_{\delta B_{i,n}}$ = standard deviation of time synchronization error
$\sigma_{\delta \boldsymbol{R}^j}$ = standard deviation of ephemeris error
σ_{v^j} = standard deviation of measurement noise

Received March 18, 1996; revision received July 17, 1996; accepted for publication July 17, 1996.

*Research Associate, Department of Aeronautics and Astronautics, W. W. Hansen Experimental Physics Laboratory. Member AIAA.
†Research Associate, Department of Aeronautics and Astronautics, W. W. Hansen Experimental Physics Laboratory.
‡Ph.D. Candidate, Department of Aeronautics and Astronautics, W. W. Hansen Experimental Physics Laboratory. Student Member AIAA.
§Ph.D. Candidate, Department of Mechanical Engineering, W. W. Hansen Experimental Physics Laboratory. Student Member AIAA.
¶Research Professor, Department of Aeronautics and Astronautics, W. W. Hansen Experimental Physics Laboratory.
**Professor, Department of Aeronautics and Astronautics, W. W. Hansen Experimental Physics Laboratory. Fellow AIAA.

I. Introduction

WHILE reducing cost and complexity, the global positioning system (GPS)[1,2] is expected to greatly improve the accuracy of navigation for land, marine, and aircraft users. However, aircraft use of GPS raises significant concern with respect to integrity, reliability, time availability, and accuracy because GPS in its current state fails to meet all four of the cited required navigation performance parameters. The wide-area augmentation system (WAAS) is tailored to meet all of them.

The WAAS is a safety-critical navigation system that adds a signal in space and an independent ground network to GPS. When it first becomes operational in 1998, it will be a supplemental system for enroute through precision approach air navigation. In time, it will become a primary navigation sensor. The WAAS will augment GPS with the following three services: a ranging function, which improves availability and reliability; differential GPS corrections, which improve accuracy; and integrity monitoring, which improves safety.

The WAAS concept is shown in Fig. 1. As shown, it broadcasts GPS integrity and correction data to GPS users and also provides a ranging signal that augments GPS. At present, a test WAAS signal is being broadcast from the geostationary International Maritime Satellite-2 (INMARSAT-2) satellite over the western portion of the Atlantic (AOR-W). This test signal has been used to broadcast differential corrections, integrity information, and a preliminary form of the ranging signal.[3,4] In 1998, the WAAS signal will be broadcast to users from the geostationary INMARSAT-3 satellites.

The ground network shown in Fig. 1 develops the differential corrections and integrity data that are broadcast to the users. Wide-area reference stations (WRSs) are widely dispersed data collection sites that receive and process signals received from the GPS and geostationary satellites. The WRSs forward their data to data processing sites referred to as wide-area master stations (WMSs).

The WMSs process the raw data to determine integrity, three-dimensional ephemeris error and satellite clock error, mostly selective availability (SA), for each monitored satellite, and vertical ionospheric delay over the continental United States. Taken together,

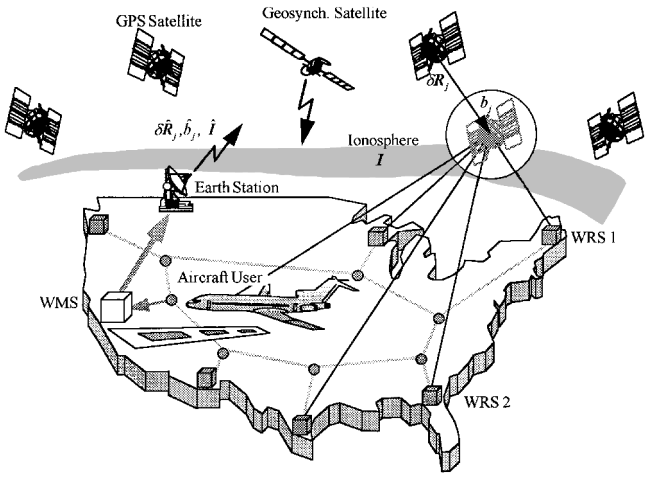

Fig. 1 Overview of WAAS.

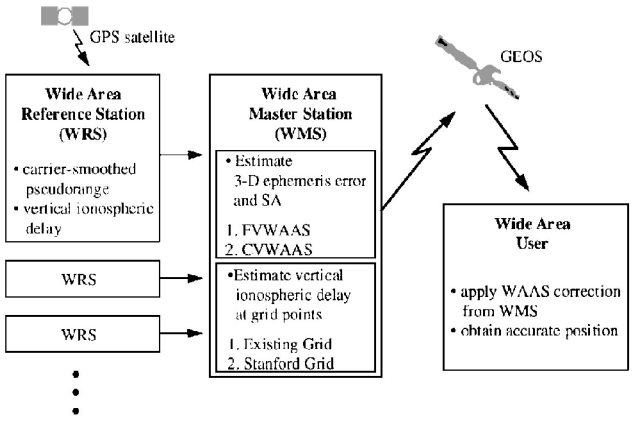

Fig. 2 Block diagram of WAAS.

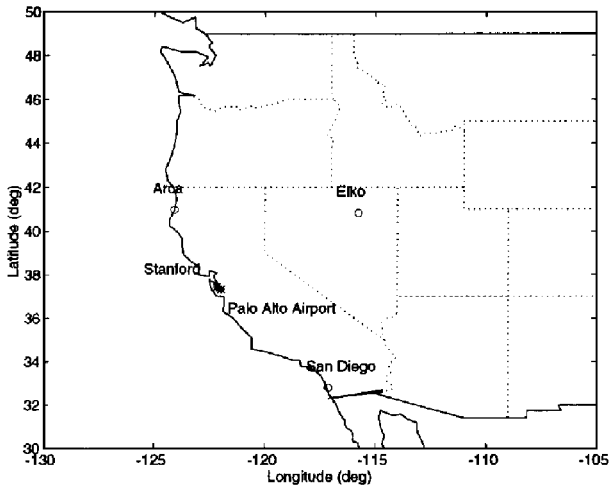

Fig. 3 Map of WRSs and WAAS users.

the differential corrections and the improved geometry provided by the geostationary satellites will improve user accuracy to better than 7.6 m (95%) in the vertical, which is adequate for aircraft category I precision approach. A simple block diagram of WAAS is shown in Fig. 2.

We mostly focus on the core algorithms to estimate the differential corrections. In the first section we compare two different WAAS algorithms to estimate three-dimensional ephemeris error and SA, which were developed at Stanford University.[4,5] In the second section we introduce the use of ionosphere measurement noise to the existing grid ionosphere estimation[6] to reduce estimation error caused by low elevation angle satellites. In the third section we apply a similar concept to WAAS user position calculation by introducing pseudorange measurement noise and a weighted least-square solution. The following sections show the static and dynamic test results using the testbed constructed by Stanford University, which is used for developing early operational experience with the WAAS and for the development and testing of new WAAS algorithms. As shown in Fig. 3, it includes WRSs located at Elko, San Diego, and Arcata in addition to WAAS static user (Stanford University) and dynamic user (Palo Alto Airport) locations.

II. Three-Dimensional Ephemeris and Clock Error Estimation

The GPS navigation message broadcast by the satellites provides a means for computing the satellite positions in the WGS-84 coordinate system.[7] These reported positions are in error due to the limitations of the GPS control segment's ability to predict the satellite ephemeris, and potentially also due to intentional degradation of the reported parameters under SA, although this is not currently observed. Also the satellite clock errors are in error mainly due to SA. The GPS satellite ephemeris and clock errors can be estimated through a network of WRSs by essentially using GPS upside down. Just as a user can determine its position and clock bias based on the ranges to the known locations of four or more GPS satellites, four or more WRSs viewing the same satellite from known locations can be used to estimate the satellite positions, satellite clock errors, and WRSs' clock errors. Even if the number of WRSs is fewer than four, a minimum norm solution can be used to estimate the errors.[8] In this case, the estimates may not be close to the true errors, but as long as the projection of those errors to the user range is close to the true range errors the WAAS corrections are still valuable.

There are two different ephemeris and SA estimation algorithms that were developed at Stanford University: full vector WAAS (FVWAAS) and common view WAAS (CVWAAS) and the following subsections describe them in order.

A. FVWAAS

The FVWAAS algorithm collects all of the measurements from the WRSs, stacks them together in one large matrix, and solves the satellite ephemeris and clock errors of all of the GPS satellites in view. The following is a detailed description of FVWAAS algorithm.

A general GPS observation equation for pseudorange (ρ_i^j) from ith WRS (subscript) to jth satellite (superscripts) is

$$\rho_i^j = d_i^j + i_i^j + t_i^j + m_i^j - \tilde{b}^j + B_i + \eta_i^{j^k} \tag{1}$$

The pseudorange residual $\delta\rho_i^j$ from ith station to jth GPS satellite, after being adjusted for broadcast ephemeris, broadcast satellite clock, ionospheric error, and tropospheric error, is modeled by

$$\delta\rho_i^j = \delta\boldsymbol{R}^j \cdot \boldsymbol{e}_i^j - b^j + B_i + v_i^j \tag{2}$$

Define $\boldsymbol{x}$ for all of the WRSs ($i = 1, \ldots, n$) and GPS satellites ($j = 1, \ldots, m$) as follows:

$$\boldsymbol{x} = [\delta\boldsymbol{R}^T \quad \boldsymbol{b}^T \quad \boldsymbol{B}^T]^T \tag{3}$$

where

$$\delta\boldsymbol{R} = \left[\delta\boldsymbol{R}_1^T \quad \delta\boldsymbol{R}_2^T \quad \cdots \quad \delta\boldsymbol{R}_m^T\right]^T$$

$$\boldsymbol{b} = [b^1 \quad b^2 \quad \cdots \quad b^m]^T, \qquad \boldsymbol{B} = [B_1 \quad B_2 \quad \cdots \quad B_{n-1}]^T$$

The matrix $\boldsymbol{B}$ has only $(n-1)$ clock terms because all of the clock errors are relative and are estimated on the basis of the nth WRS clock.

If we gather all of the measurement equations for all of the WRSs ($i = 1, \ldots, n$) and GPS satellites ($j = 1, \ldots, m$) and rearrange them, we will get a matrix equation as follows:

$$\begin{bmatrix} \boldsymbol{E}_1 & -\boldsymbol{I} & \boldsymbol{I}_1 \\ \boldsymbol{E}_2 & -\boldsymbol{I} & \boldsymbol{I}_2 \\ \vdots & \vdots & \vdots \\ \boldsymbol{E}_n & -\boldsymbol{I} & \boldsymbol{I}_n \end{bmatrix} \boldsymbol{x} = \boldsymbol{\delta D} \tag{4}$$

where

$$\boldsymbol{E}_i = \begin{bmatrix} \boldsymbol{e}_i^{1^T} & \mathbf{0} & \mathbf{0} & \mathbf{0} \\ \mathbf{0} & \boldsymbol{e}_i^{2^T} & \mathbf{0} & \mathbf{0} \\ \mathbf{0} & \mathbf{0} & \ddots & \mathbf{0} \\ \mathbf{0} & \mathbf{0} & \mathbf{0} & \boldsymbol{e}_i^{m^T} \end{bmatrix} \qquad (m \times 3m)$$

$$\boldsymbol{I} = \begin{bmatrix} 1 & 0 & 0 & 0 \\ 0 & 1 & 0 & 0 \\ 0 & 0 & \ddots & 0 \\ 0 & 0 & 0 & 1 \end{bmatrix} \qquad (m \times m)$$

(ith column)

$$\boldsymbol{I}_i = \begin{bmatrix} 0 & \cdots & 1 & \cdots & 0 \\ 0 & \cdots & 1 & \cdots & 0 \\ \vdots & \cdots & \vdots & \cdots & \vdots \\ 0 & \cdots & 1 & \cdots & 0 \end{bmatrix} \qquad [m \times (n-1)]$$

(for $i = 1, \ldots, n-1$)

$$\boldsymbol{I}_n = \mathbf{0} \qquad [m \times (n-1)] \qquad (\text{for} \quad i = n)$$

$$\boldsymbol{\delta D} = [\boldsymbol{\delta D}_1 \quad \boldsymbol{\delta D}_2 \quad \cdots \quad \boldsymbol{\delta D}_n]^T$$

$$\boldsymbol{\delta D}_i = \left[\delta\rho_i^1 \quad \delta\rho_i^2 \quad \cdots \quad \delta\rho_i^m\right]^T$$

In the preceding equations the matrix $\boldsymbol{I}_n$ is set to be $\mathbf{0}$ matrix because all of the clock errors are relative and are estimated on the basis of the nth WRS clock as explained earlier. If we define the system matrix $\boldsymbol{H}$ and measurement z as

$$\boldsymbol{H} = \begin{bmatrix} \boldsymbol{E}_1 & -\boldsymbol{I} & \boldsymbol{I}_1 \\ \boldsymbol{E}_2 & -\boldsymbol{I} & \boldsymbol{I}_2 \\ \vdots & \vdots & \vdots \\ \boldsymbol{E}_n & -\boldsymbol{I} & \boldsymbol{I}_n \end{bmatrix} \tag{5}$$

$$z = \boldsymbol{\delta D} \tag{6}$$

then Eq. (4) becomes

$$z = \boldsymbol{H}\boldsymbol{x} \tag{7}$$

In the case that the ith WRS cannot see the jth satellite, the corresponding row element of the vector z and row vector of the matrix $\boldsymbol{H}$ in Eq. (5) must be eliminated.

The WMS can use a sequential filter or a batch least-squares technique to estimate the three-dimensional ephemeris error vector and clock bias for each GPS satellite within view of the network. The latter was used. If there are more measurements than the unknowns (three-dimensional ephemeris errors, satellite clock error, and WRS clock error) in the WAAS network, the observation equation for that satellite is overdetermined, and the solution is picked to minimize the measurement residual sum of squares:

$$\boldsymbol{x} = (\boldsymbol{H}^T\boldsymbol{H})^{-1}\boldsymbol{H}^T z \tag{8}$$

If there are fewer measurements than unknowns, the solution is underdetermined, and the optimal estimate minimizes the two norm of the error solution:

$$\boldsymbol{x} = \boldsymbol{H}^T(\boldsymbol{H}\boldsymbol{H}^T)^{-1}z \tag{9}$$

In the underdetermined case, the corrections for ephemeris errors and clock offsets are not accurate, but the user positioning is still accurate with these corrections because for the user only the projection of the error correction vector on the line of sight to the satellite is important.

The FVWAAS algorithm runs slowly because it needs to manipulate relatively large matrices but the estimation errors, especially WRS's clock estimation errors, depend only on the measurement noise. The processing speed and the memory requirement of the algorithm can be greatly improved using a sparse matrix manipulation technique[9] because 90% of elements in the observation matrix $\boldsymbol{H}$ are zeros.

B. CVWAAS

Instead of stacking all of the measurements in one large matrix as the FVWAAS the CVWAAS decouples the measurements for each satellite by synchronizing all of the clocks in WRSs using the well-known common view time transfer technique,[10] and estimates three-dimensional ephemeris error and SA for each satellite. The following is the detailed description of CVWAAS algorithm.

Common view time transfer differences the pseudorange residuals from two sites as follows:

$$\delta\rho_{i,n}^j \equiv \delta\rho_i^j - \delta\rho_n^j = \delta\boldsymbol{R}^j \cdot \left(\boldsymbol{e}_i^j - \boldsymbol{e}_n^j\right) + B_{i,n} + v_{i,n}^j \tag{10}$$

where $B_{i,n} = B_i - B_n$.

If the line-of-sight difference is small or the ephemeris error is small and random, a good estimate of the clock difference can be achieved as follows:

$$\hat{B}_{i,n} = \frac{1}{l_{i,n}} \sum_{j=1}^{l_{i,n}} \delta\rho_{i,n}^j = B_{i,n} + \delta B_{i,n} \tag{11}$$

$$\sigma_{\delta B_{i,n}} = \frac{\sqrt{\sigma_{\delta\boldsymbol{R}^j}^2 + \sigma_{v^j}^2}}{\sqrt{l_{i,n}}} \tag{12}$$

If the two sites are perfectly synchronized, then $\delta B_{i,n}$ is zero. From now on we assume the perfect time synchronization of all of the WRSs for the purpose of the derivation. The clock estimate of WRS is then used to eliminate the receiver clock error term in Eq. (2). Thus we have all of the measurements in terms of a common clock. The synchronized pseudorange residuals are described as follows:

$$\delta\tilde{\rho}_i^j = \delta\rho_i^j - \hat{B}_{i,n} = \delta\boldsymbol{R}^j \cdot \boldsymbol{e}_i^j - b^j + B_n + v_i^j \tag{13}$$

These synchronized pseudorange residuals are the fundamental inputs to the CVWAAS satellite ephemeris and clock estimation algorithms. The three-dimensional ephemeris error solution begins by differencing pairs of synchronized pseudorange residuals as follows:

$$\delta\tilde{\rho}_{i,n}^j = \delta\tilde{\rho}_i^j - \delta\tilde{\rho}_n^j = \delta\boldsymbol{R}^j \cdot \left(\boldsymbol{e}_i^j - \boldsymbol{e}_n^j\right) + v_{i,n}^j \tag{14}$$

This set of single differences does not contain the satellite clock offsets, and each satellite is now decoupled. The three-dimensional ephemeris error for each satellite may be estimated using the following set of observation equations:

$$\begin{bmatrix} \delta\tilde{\rho}_{1,n}^j \\ \vdots \\ \delta\tilde{\rho}_{n-1,n}^j \end{bmatrix} = \begin{bmatrix} \left(\boldsymbol{e}_1^j - \boldsymbol{e}_n^j\right) \\ \vdots \\ \left(\boldsymbol{e}_{n-1}^j - \boldsymbol{e}_n^j\right) \end{bmatrix} \delta\boldsymbol{R}^j \tag{15}$$

The linear system of equations can be written more compactly by defining z and $\boldsymbol{H}$ such that

$$z = \boldsymbol{H} \cdot \delta\boldsymbol{R}^j \tag{16}$$

where

$$z = \begin{bmatrix} \delta\tilde{\rho}_{1,n}^j \\ \vdots \\ \delta\tilde{\rho}_{n-1,n}^j \end{bmatrix}, \qquad \boldsymbol{H} = \begin{bmatrix} \left(\boldsymbol{e}_1^j - \boldsymbol{e}_n^j\right) \\ \vdots \\ \left(\boldsymbol{e}_{n-1}^j - \boldsymbol{e}_n^j\right) \end{bmatrix}$$

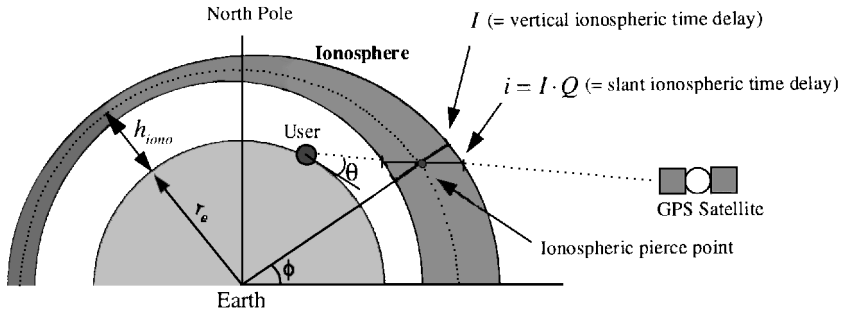

Fig. 4 Ionospheric time delay observation.

A least-square solution or a minimum-norm solution can be used to generate the ephemeris error estimate $\delta\hat{\boldsymbol{R}}^j$, which is the same way as FVWAAS but with a smaller matrix,

$$\delta\hat{\boldsymbol{R}}^j = \boldsymbol{H}^T(\boldsymbol{H}\boldsymbol{H}^T)^{-1}\boldsymbol{z} \tag{17}$$

$$\delta\hat{\boldsymbol{R}}^j = (\boldsymbol{H}^T\boldsymbol{H})^{-1}\boldsymbol{H}^T\boldsymbol{z} \tag{18}$$

By substituting the ephemeris error estimate back into Eq. (13), the satellite clock error estimate is obtained. If we assume that we know the master clock perfectly (i.e., $B_n = 0$), then we obtain the satellite clock estimate as follows:

$$\hat{b}^j = \frac{1}{n}\sum_{i=1}^{n}\left(\delta\hat{\boldsymbol{R}}^j \cdot \boldsymbol{e}_i^j - \delta\tilde{\rho}_i^j\right) \tag{19}$$

Even if the master clock is not known it does not cause degradation in WAAS user navigation accuracy because all of the satellite clock errors have the common clock error and, therefore, they will be absorbed into the user clock error.

The CVWAAS algorithm is fast and requires relatively little mathematical computation and memory. But as indicated in Eqs. (11) and (12), it can be sensitive to the ephemeris errors due to the limitations of the GPS control segment's ability to predict the satellite ephemeris as well as the measurement noise. However, applying sequential filter methods with appropriate orbit model can improve filter performance.[11]

III. Vertical Ionospheric Time Delay Estimation

As GPS satellite signals traverse the ionosphere, their modulation is delayed by an amount proportional to the number of free ions encountered. This is known as ionospheric time delay. The ionospheric time delay is a function of local time, magnetic latitude, sunspot cycle, and other factors. Its highest peak occurs at about 2:00 p.m. local solar time. The basics of ionospheric time delay are shown in Fig. 4. Klobuchar[12] developed a simple analytical model for ionospheric time delay and of which parameters are being broadcast for single frequency user to correct the ionospheric time delay.

The WMS processes the vertical ionospheric delay data for all ionospheric pierce points from the WRSs to generate a grid of vertical ionospheric grid estimates as described in Ref. 13, which uses the following grid algorithm (a kind of a weighted interpolation technique):

$$\hat{I}_{\text{Grid},V} = I^{\text{Grid}}_{\text{Klob},V}\left\{\left[\sum_{k=1}^{K}\left(\frac{I^k_{\text{Meas},V}}{I^k_{\text{Klob},V}}\right)\cdot w^k\right]\Big/\sum_{n=1}^{K} w^n\right\} \tag{20}$$

where w^k is weight of kth ionosphere pierce point.

The ionospheric pierce points are the points where the signals from GPS satellites intersect the imaginary sphere 350 km above the Earth's surface, which is the average height of ionosphere as assumed in this paper. The ionospheric pierce points and the grid points are shown in Fig. 5. The grid used is uniform in latitude and longitude with points every five degrees. This grid point estimates will be interpolated to estimate the vertical ionospheric delay for each satellite at the WAAS user.

The existing grid algorithm[13] uses only the inverse of the distance from the grid point to the pierce point as weight,

$$w^k = 1/d^k \tag{21}$$

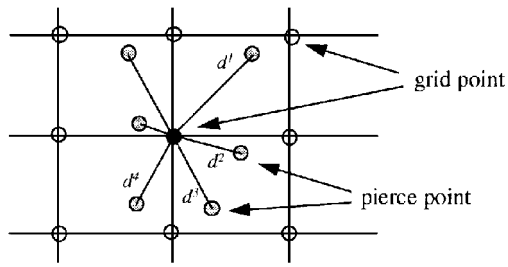

Fig. 5 Ionospheric pierce point and grid.

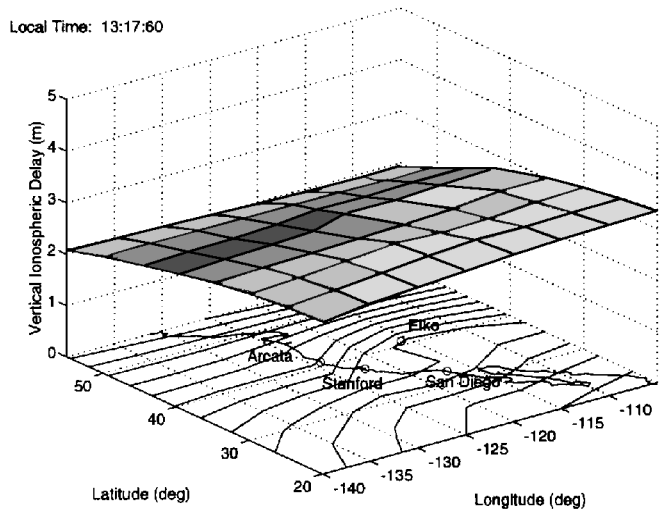

Fig. 6 Estimated vertical ionosphere surface (ionospheric correction at each grid point as a surface plot and the corresponding contour lines on top of the map for one instant in time).

The longer the distance between the pierce point and the grid point is the less correlation between the ionospheric delay measurement at the pierce point and the ionospheric estimate at the grid point is. Adding estimates of ionosphere measurement noise to the weight can reduce unexpected jumps in the ionospheric estimate especially when a new satellite is rising because large measurement noise usually occurs for a low elevation angle satellite. We developed an empirical formula to combine the distance and the measurement noise into the weight for the pierce point as follows:

$$\begin{aligned} w^k &= \left[\{f(d^k)\}^2 + \{f(v^k)\}^2\right]^{-\frac{1}{2}} \\ &= \left[\left\{\left(\frac{d^k}{200\,\text{km}}\right)^{\frac{3}{4}}\right\}^2 + (v^k)^2\right]^{-\frac{1}{2}} \end{aligned} \tag{22}$$

where v^k in meters depends on elevation angle, multipath environment, carrier smoothed filter, receiver noise, etc. Using the Stanford modified grid algorithm we can obtain a real-time estimate of the ionosphere surface. An example of this surface is shown in Fig. 6.

As may be seen in the static test section, this Stanford grid algorithm reduces the maximum vertical positioning error of the WAAS user. However, the preceding empirical formula (22) needs to be further tuned and verified using a larger set of data.

IV. Weighted Least-Square Solution in WAAS User

A technique similar to the one described in the preceding section can improve the WAAS user navigation accuracy. As is known, measurement noise for a low elevation satellite is higher than that for a high elevation satellite[14,15] because of low signal-to-noise ratio, big multipath, etc. A weighted least-square technique can be introduced to take this into account.

The pseudorange residual $\delta\rho^j$ from WAAS user to jth GPS satellite, already adjusted for broadcast ephemeris, broadcast satellite clock, tropospheric error, and WAAS corrections, is modeled by

$$\delta\rho^j = -\boldsymbol{R}_u \cdot \boldsymbol{e}^j + B + v^j \tag{23}$$

If we gather all of the measurement equations (23) for all of the satellites in view and rearrange them, we will get a matrix equation as follows:

$$z = \boldsymbol{H}\boldsymbol{x} + \boldsymbol{v} \tag{24}$$

where

$$z = \begin{bmatrix} -\delta\rho^1 \\ \vdots \\ -\delta\rho^m \end{bmatrix}, \qquad \boldsymbol{H} = \begin{bmatrix} \boldsymbol{e}^{1^T} & -1 \\ \vdots & \vdots \\ \boldsymbol{e}^{m^T} & -1 \end{bmatrix}$$

$$\boldsymbol{x} = \begin{bmatrix} \boldsymbol{R}_u \\ B \end{bmatrix}, \qquad \boldsymbol{v} = \begin{bmatrix} -v^1 \\ \vdots \\ -v^m \end{bmatrix}$$

Then a weighted least-square technique using the sensor covariance matrix, $\boldsymbol{V} = E[\boldsymbol{v} \cdot \boldsymbol{v}^T]$, is applied to obtain the user position and receiver clock error as follows:

$$\boldsymbol{x} = (\boldsymbol{H}^T\boldsymbol{V}^{-1}\boldsymbol{H})^{-1}\boldsymbol{H}^T\boldsymbol{V}^{-1}z \tag{25}$$

Because multipath has time constant from 5–30 min and the magnitude of multipath and receiver noise are bigger for a low elevation satellite than for a high elevation satellite, this generates slowly moving bias and jumps in user position solution. The weighted least-square solution reduces these bias and jumps effectively by reducing the weight of the low elevation satellite.

V. Static Tests

Static tests were conducted for 24 h using the Stanford real-time experimental WAAS network on July 21, 1994. The Stanford real-time experimental WAAS network has three WRS sites and one user site, all of which are equipped with weather stations, rubidium clocks, and Trimble 4000SSE dual-frequency receivers. The map of the sites and the baseline information are in Fig. 3 and Table 1, respectively. The minimum baseline from the static user (Stanford) to WRS (Arcata) is 427 km. The locations of the four antennas have been independently measured using standard GPS surveying techniques. The locations have been accurately found in the International Terrestrial Reference Frame (ITRF)-92, and the relative baselines are self-consistent to the 2-cm level. For the static user we did not use ionospheric measurement from the dual-frequency receiver but used only L1 frequency information to make it a single-frequency WAAS user. Sampling time for all of the WRSs was 30 s, and SA was on during the test. All of the data were postprocessed on snapshot basis as if they had been in real time. Because the sampling time is 30 s, the positioning accuracy with 6-s latency was depicted using SA statistics assuming that WAAS user computes the rate of correction based on the prior corrections and predicts the correction for the current epoch using the prior correction and its rate information.[4]

Table 1 Baseline from WAAS user to WRSs

WRS	From Stanford, km
Arcata, CA	427
Elko, NV	669
San Diego, CA	687

Table 2 Static WAAS user positioning errors for different algorithms (July 21, 1994, in meters)

		Zero latency			6-s latency,
		East–West	North–South	Vertical	vertical
Stand-alone user	95	32.5	37.4	79.6	79.6
position error, %	max	63.6	92.2	190.6	——
FVWAAS with	95	1.35	1.26	2.80	2.98
existing iono., %	max	1.52	1.76	5.81	——
FVWAAS with	95	1.40	1.26	2.84	3.02
Stanford iono., %	max	1.52	1.75	3.83	——
CVWAAS with	95	1.73	1.51	3.30	3.48
existing iono., %	max	2.72	1.94	4.89	——

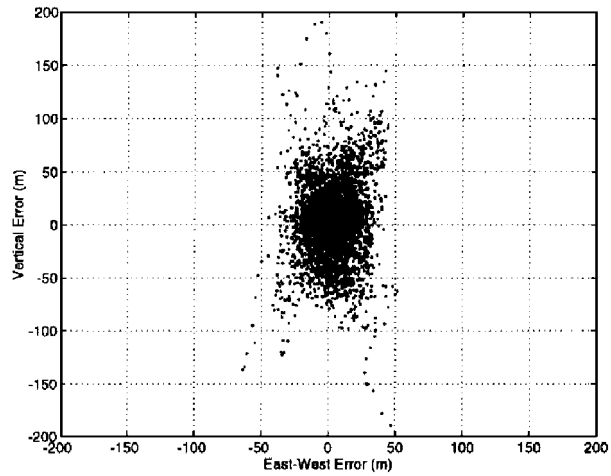

Fig. 7 Vertical stand-alone user positioning errors (July 21, 1994, 24 h).

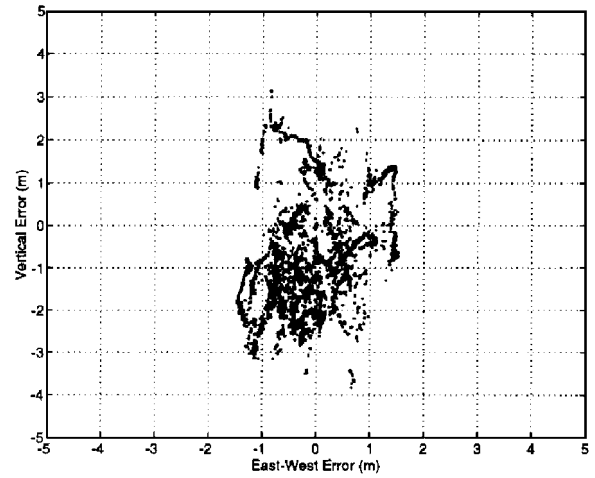

Fig. 8 Vertical FVWAAS user positioning errors (July 21, 1994, 24 h).

The vertical positioning errors of the stand-alone user are computed and shown in Fig. 7. We ran the tests for three different configurations to compare the performance of each WAAS algorithm, and the results are summarized in Table 2. The first test is using the FVWAAS for ephemeris and SA estimation and the existing grid algorithm for ionosphere estimation.[6] The second test is using FVWAAS and the Stanford modified grid algorithm and the results are shown in Fig. 8. The third test is using CVWAAS and the existing grid algorithm and the results are shown in Fig. 9.

Table 2 indicates that all of the three different configurations with zero and 6-s latency give 3.3 and 3.5 m of WAAS user rms vertical

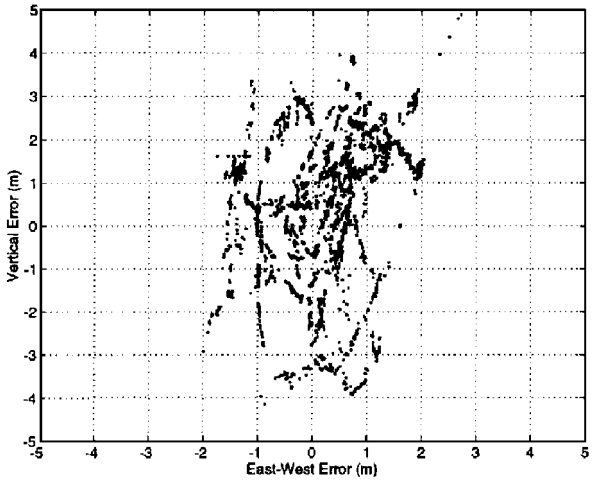

Fig. 9 Vertical CVWAAS user positioning errors (July 21, 1994, 24 h).

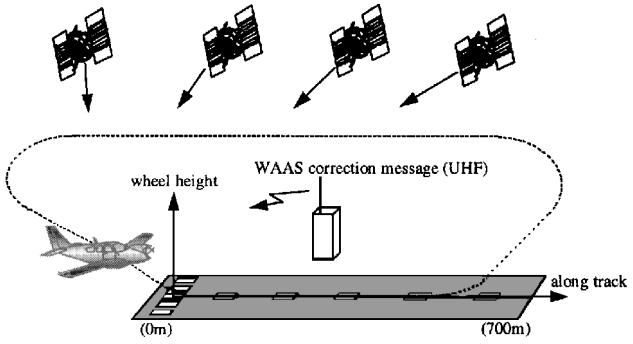

Fig. 10 Runway coordinate.

positioning error, respectively, compared to 80 m for stand-alone user. These results are better than the category I instrument landing system (ILS) 95% navigation sensor error limits of 4.1 m in vertical.

The first and the second test results can provide the performance comparison between the Stanford and the existing ionosphere estimation algorithms. Table 2 shows that the overall rms value of vertical positioning error is about the same (2.8 m) for both the Stanford and the existing algorithms, but the Stanford modified grid algorithm reduces the maximum WAAS user vertical positioning error about 30% (3.83 m) compared with the existing grid algorithm (5.81 m). Typically, ionospheric errors have a greater impact on vertical positioning than horizontal positioning.

Because both the first and the second configurations use the existing grid algorithm the test results can provide the performance comparison between FVWAAS and CVWAAS. Table 2 shows that the FVWAAS algorithm improves the WAAS user rms vertical positioning error about 15% (2.8 m) compared with the CVWAAS algorithm (3.3 m). This is because the CVWAAS has an extra WRS clock synchronization error due to ephemeris errors.

VI. Dynamic Tests

Dynamic tests were conducted at Palo Alto airport near Stanford University using the same three Stanford real-time experimental WRSs used for the static tests at 3:20 p.m. on Dec. 21, 1994. A total of four landings and takeoffs were performed. The map of the WRSs and the airport are shown in Fig. 3.

The GSV-1002 single-frequency receiver was installed in the Piper Dakota airplane and the weather information available at the airport was applied before the flight tests. During the flight test WAAS correction was generated and transmitted to the airplane via uhf link. As a truth source we have used the surveyed location of the runway at Palo Alto airport, where we have applied a flat runway model. A previous survey confirms that this approximation should be accurate to better than 1 m (Ref. 16). The centerline at the desired touchdown point of the runway (55 m from the start) is taken as the local origin, and the total length of the runway is just over 760 m. The coordinate of the runway is shown in Fig. 10.

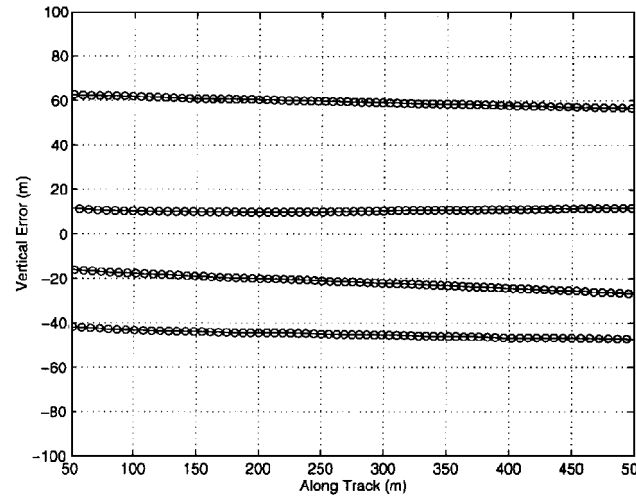

Fig. 11 Vertical positioning errors of the stand-alone aircraft user (3:20 p.m. in local time, Dec. 21, 1994, four landings and takeoffs).

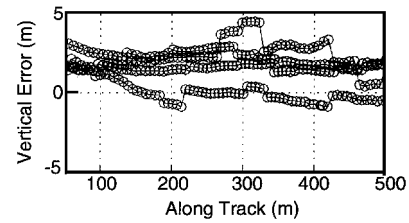

Fig. 12 Perfect datalink. The vertical positioning errors of the aircraft user (FVWAAS, 3:20 p.m. in local time, Dec. 21, 1994, without weighted least-square in WAAS user position calculation, four landings and takeoffs).

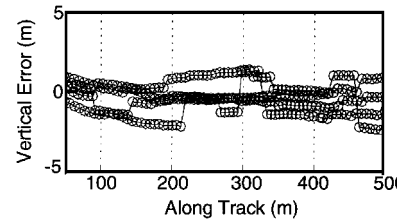

Fig. 13 Perfect datalink. The vertical positioning errors of the aircraft user (FVWAAS, 3:20 p.m. in local time, Dec. 21, 1994, with weighted least-square in WAAS user position calculation, four landings and takeoffs).

The flight data were collected near after the peak ionospheric period in real time at 1-Hz rate for WRSs and at 5 Hz for an airborne user. We postprocessed the flight data as if these were real-time flight tests. Because the corrections are applied at the 250-bps rate[17] there is a resulting latency in the WAAS corrections of up to 6 s. In the airborne user the current correction is generated with a simple velocity model from two previous corrections.

The vertical errors of the stand-alone aircraft user on the runway are plotted in Fig. 11, and the errors are between ± 70 m mainly because of SA. We ran the tests for three different configurations to compare the performance of each algorithm, and the vertical errors of the aircraft user on the runway are plotted in Figs. 12 and 13. All of the tests used the existing grid ionosphere estimation algorithm. The first test used the FVWAAS and the simple least-square solution for the airborne user, and the results are shown in Fig. 12. The second test used FVWAAS and the weighted least-square solution for the airborne user, and the results are shown in Fig. 13. The third test used CVWAAS and the weighted least-square solution for the airborne user, and the results are very similar to the second test and therefore are not shown.

For each of the landings and takeoffs it is safe to assume that the wheels of the airplane were on the runway from roughly 50 to 500 m from the desired touchdown point. In Fig. 12 there is a bias in the vertical positioning errors because of the runway-reflected multipath

due to the low elevation satellite, which effect is similar to adding noise, bias, and jumps to pseudorange measurement, and this bias does not appear in Fig. 13, which uses the weighted least-square solution. The weighted least-square solution technique reduces the multipath effect by lowering the weight of the noisy pseudorange measurement from the low elevation satellite. In Fig. 13 the vertical positioning errors are ±2.5 m, which is well within the ±4.1-m 95% error limits for a category I ILS landing system. These flight test results indicate that both FVWAAS and CVWAAS are qualified for real-time WAAS operation. These results might be a little optimistic considering that the solar activity, which was low during the year the flight tests were performed, will increase up to three times the current value during maximum solar cycle. But the ionosphere estimation error will increase at lower magnitude,[18] and we believe that the requirement for category I precision approach will still be met.

VII. Conclusions

We compared two different WAAS algorithms for ephemeris error and satellite clock error estimation, FVWAAS and CVWAAS. Both the static and dynamic test results showed that better than 3.5 m of WAAS user vertical positioning accuracy can be achieved using the FVWAAS or CVWAAS algorithm even with 6-s latency, which is well within the ±4.1-m 95% error limits for a category I ILS landing system. Both algorithms are qualified for real-time WAAS operation, and the algorithm has to be chosen based on available processing power and accuracy requirement. We introduced the Stanford modified grid ionosphere estimation algorithm that takes into account the ionosphere measurement noise as well as the distance from the grid to the ionospheric pierce point, and the static test results indicated that it reduces the maximum WAAS vertical positioning error about 30% (3.83 m) compared with the existing grid algorithm (5.81 m). The flight test results showed that the weighted least-square solution reduces bias and jumps that are due to multipath of low elevation satellite in WAAS user positioning errors.

Acknowledgments

The authors gratefully acknowledge the support and assistance of AGS-100 (the satellite program office). They also acknowledge help from A. J. Van Dierendonck, Jeffrey Freymueller, Juan Ceva, Andrew Barrows, Jennifer Evans, Eric Abbott, and David Powell.

References

[1]Parkinson, B. W., Spillker, J., Jr., Axelrad, P., and Enge, P. (eds.), *The Global Positioning System: Theory and Applications*, Volume 1, AIAA, Washington, DC, 1996.

[2]Parkinson, B. W., Spillker, J., Jr., Axelrad, P., and Enge, P. (eds.), *The Global Positioning System: Theory and Applications*, Volume 2, AIAA, Washington, DC, 1996.

[3]Haas, F. M., and Lage, M. E., "GPS Wide-Area Augmentation System (WAAS) Testbed Results—Phase 1D Testbed Results," *Proceedings of the 50th Annual Meeting of the Institute of Navigation* (Colorado Springs, CO), Inst. of Navigation, Alexandria, VA, 1994, pp. 239–248.

[4]Kee, C., and Parkinson, B. W., "Wide-Area Differential GPS as a Future Navigation System in the U. S.," *Proceedings of IEEE PLANS'94* (Las Vegas, NV), Inst. of Electrical and Electronics Engineers, Piscataway, NJ, 1994, pp. 778–795.

[5]Walter, T., Kee, C., Chao, Y. C., Tsai, Y. J., Peled, U., Ceva, J., Barrows, A. K., Abbot, E., Powell, D., Enge, P., and Parkinson, B. W., "Flight Trials of the Wide-Area Augmentation System (WAAS)," *Proceedings of the Institute of Navigation GPS-94* (Salt Lake City, UT), Inst. of Navigation, Alexandria, VA, 1994, pp. 1537–1546.

[6]El-Arini, M. B., O'Donnell, P. A., Kellam, P. M., Klobuchar, J. A., Wisser, T. C., and Doherty, P. J., "The FAA Wide-Area Differential GPS (WADGPS) Static Ionospheric Experiment," *Proceedings of the 1993 National Technical Meeting of the Institute of Navigation* (San Francisco, CA), Inst. of Navigation, Alexandria, VA, 1993, pp. 485–496.

[7]Green, G. B., Massatt, P. D., and Rhodus, N. W., "The GPS 21 Primary Satellite Constellation," *NAVIGATION, Journal of the Institute of Navigation*, Vol. 36, No. 1, 1989, pp. 9–24.

[8]Kee, C., Parkinson, B. W., and Axalrad, P., "Wide-Area Differential GPS," *NAVIGATION, Journal of the Institute of Navigation*, Vol. 38, No. 2, 1991, pp. 123–145.

[9]Gilbert, J. R., Moler, C., and Schreiber, R., "Sparse Matrices in MATLAB: Design and Implementation," *SIAM Journal on Matrix Analysis*, Vol. 13, No. 1, 1992, pp. 333–356.

[10]Allan, D. W., and Weiss, M. A., "Accurate Time and Frequency Transfer During Common-View of a GPS Satellite," *Proceedings of 34th Annual Frequency Control Symposium*, U.S. Army Electronics Research and Development Command, Ft. Monmouth, NJ, 1980, pp. 334–346.

[11]Tsai, Y. J., Chao, Y. C., Walter, T., Kee, C., Powell, D., Enge, P., and Parkinson, B. W., "Evaluation of Orbit and Clock Models for Real Time WAAS," *Proceedings of the Institute of Navigation 1995 National Technical Meeting*, Inst. of Navigation, Alexandria, VA, 1995, pp. 539–547.

[12]Klobuchar, J., "Ionospheric Time-Delay Algorithm for Single-Frequency GPS Users," *IEEE Transactions on Aerospace and Electronic Systems*, Vol. 23, No. 3, 1987, pp. 325–331.

[13]El-Arini, M. B., Klobuchar, J. A., and Doherty, P. H., "Evaluation of the GPS WAAS Ionospheric Grid Algorithm During the Peak of the Current Solar Cycle," *Proceedings of the Institute of Navigation 1994 National Technical Meeting*, Inst. of Navigation, Alexandria, VA, 1994, pp. 961–968.

[14]Kee, C., Walter, T., Enge, P., and Parkinson, B. W., "Quality Control Algorithms on Wide-Area Reference Station for WAAS," *Proceedings of the 52nd Institute of Navigation (ION) Annual Meeting* (Cambridge, MA), Inst. of Navigation, Alexandria, VA, 1996, pp. 487–495.

[15]Walter, T., and Enge, P., "Weighted RAIM for Precision Approach," *Proceedings of the Institute of Navigation GPS-95*, Inst. of Navigation, Alexandria, VA, 1995, pp. 1995–2004.

[16]Cohen, C. E., Pervan, B. S., Lawrence, D. G., Cobb, H. S., Powell, J. D., and Parkinson, B. W., "Real-Time Flight Test Evaluation of the GPS Marker Beacon Concept for Category III Kinematic GPS Precision Landing," *Proceedings of the Institute of Navigation GPS-93* (Salt Lake City, UT), Inst. of Navigation, Alexandria, VA, 1993, pp. 841–849.

[17]Van Dierendonck, A. J., and Enge, P. K., "The Wide-Area Augmentation System (WAAS) Signal Specification," *Proceedings of the Institute of Navigation GPS-94*, Inst. of Navigation, Alexandria, VA, 1994, pp. 985–994.

[18]Klobuchar, J. A., Doherty, P. J., and El-Arini, M. B., "Potential Ionospheric Limitations to GPS Wide-Area Augmentation System (WAAS)," *NAVIGATION, Journal of the Institute of Navigation*, Vol. 42, No. 2, 1995, pp. 353–370.